Journal of Inorganic Biochemistry 231 (2022) 111785

Contents lists available at ScienceDirect

Journal of Inorganic Biochemistry

journal homepage: www.elsevier.com/locate/jinorgbio

Short Communication

EPR characterization of the heme domain of a self-sufficient cytochrome P450 (CYP116B5)

Antonino Famulari [a,b], Danilo Correddu [c], Giovanna Di Nardo [c], Gianfranco Gilardi [c], Mario Chiesa [b], Inés García-Rubio [a,d,*]

[a] Department of Condensed Matter Physics, University of Zaragoza, Calle Pedro Cerbuna 12, 50009 Zaragoza, Spain
[b] Department of Chemistry, University of Turin, Via Giuria 9, 10125 Torino, Italy
[c] Department of Life Sciences and Systems Biology, University of Turin, Via Accademia Albertina, 13, 10123 Turin, Italy
[d] Centro Universitario de la Defensa, Carretera de Huesca s/n, 50090 Zaragoza, Spain

ARTICLE INFO

Keywords:
Cytochromes P450
HYSCORE
EPR
Low-spin iron heme
Peroxygenase
Ferric hemeprotein

ABSTRACT

CYP116B5 is a self-sufficient cytochrome P450 (CYP450) with interesting catalytic properties for synthetic purposes. When isolated, its heme domain can act as a peroxygenase on different substrates of biotechnological interest. Here, by means of continuous wave and advanced EPR techniques, the coordination environment of iron in the isolated CYP116B5 heme domain (CYP116b5hd) is characterized. The ligand-free protein shows the characteristic EPR spectrum of a low-spin ($S = 1/2$) Fe^{III}-heme with [$g_z = 2.440 \pm 0.005$, $g_y = 2.25 \pm 0.01$, $g_x = 1.92 \pm 0.01$]. These *g*-values reflect an electronic ground state very similar to classical P450 monooxygenases rather than P450 peroxygenases. Binding of imidazole results in *g*-values very close to the ones reported for CYP152 peroxygenases. The detection of hyperfine interactions through HYperfine Sub-level CORrElation (HYSCORE) Spectroscopy experiments, shows that this is due to a nitrogen-mediated axial coordination. This work adds a piece of experimental evidence to the research, aimed at elucidating the features that distinguish the classical P450 enzymes from peroxygenases. It shows that the electronic environment of heme iron of CYP116B5 in the resting state is similar to the classical P450 monooxygenases. Therefore, it is not the critical factor that confers to CYP116B5hd its peroxygenase-like activity, suggesting a crucial role of the protein matrix.

1. Introduction

Class VII cytochromes P450 (CYP450s) are self-sufficient monooxygenases carrying a P450 domain and a phthalate family oxygenase (PFOR)-like reductase domain fused in a single polypeptide chain [1]. They are attractive targets for biocatalytic applications such as the synthesis of fine chemicals and pharmaceuticals [2–4]. Among them, CYP116B5 from *Acinetobacter radioresistens* S13, is involved in the terminal hydroxylation of n-alkanes and its isolated heme domain (CYP116B5hd) is able to carry out different oxidative reactions using the so-called peroxide shunt [5,6]. CYP116B5hd showed a higher stability towards heme damage induced by hydrogen peroxide when compared to the heme domain (BMP) of cytochrome P450 BM3 [6].

EPR is an established tool for the detailed study of the geometrical and electronic structure of metal enzymes featuring paramagnetic states and has been successfully applied to study cytochromes P450 [7–11]. Here, a deeper investigation of the electronic state of the heme iron in CYP116B5hd was carried out by means of Continuous Wave (CW)-EPR combined with HYperfine Sublevel COrRElation (HYSCORE) spectroscopy, which, in recent years, has provided a detailed description of the coordination of the metal and the electronic structure of the 3d orbitals involved in the iron–ligand bond for ferric hemeproteins [12–15].

The heme coordination environment of CYP116B5hd was explored by means of X-band CW-EPR. As expected for a ligand-free cytochrome P450, the spectrum of CYP116B5hd shows the characteristic powder pattern of a low-spin (S=1/2) Fe^{III}-heme center with three well-resolved peaks corresponding to the features of an anisotropic *g*-tensor (Fig. 1a). Down to 6 K, no signs of high-spin Fe^{III}-heme were found around 100 mT

Abbreviations: CYP450, Cytochrome P450; CYP116B5hd, CYP116B5 heme domain; HYSCORE, Hyperfine Sub-level Correlation Spectroscopy; BM3, CYPBM3 heme domain; CPO, Chloroperoxidase; CW-EPR, Continuous-Wave Electron Paramagnetic Resonance; P450, CYP450; KPi, Potassium Phosphate; UV-Vis, Ultraviolet-visible absorption spectroscopy; S.D., Supplementary data.

* Corresponding author at: Department of Condensed Matter Physics, Faculty of Sciences, University of Zaragoza, Calle Pedro Cerbuna 12, 50009 Zaragoza, Spain.
E-mail address: inesgr@unizar.es (I. García-Rubio).

https://doi.org/10.1016/j.jinorgbio.2022.111785
Received 21 August 2021; Received in revised form 25 February 2022; Accepted 26 February 2022
Available online 2 March 2022

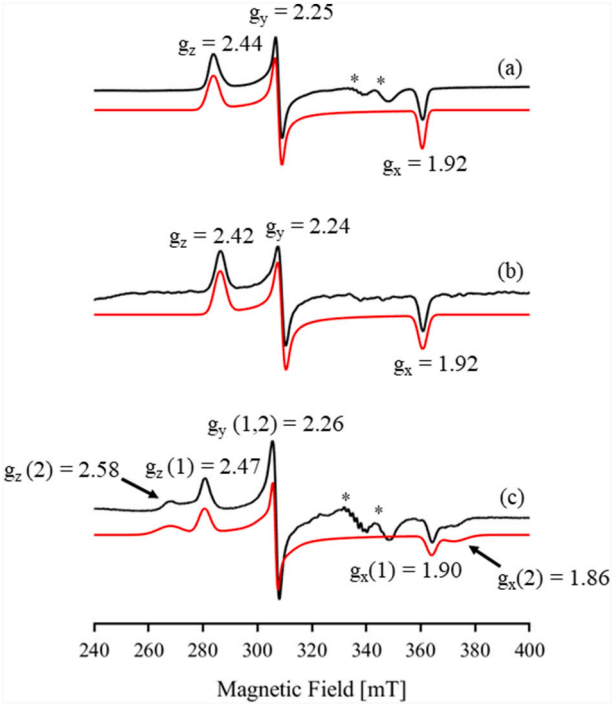

Fig. 1. Experimental (black line) and simulated (red line) X-band CW-EPR spectra of (a) CYP116B5hd in the resting state at 40 K, (b) CYP116B5hd with a 10-fold excess of histidine at 77 K and (c) CYP116B5hd with a 10-fold excess of imidazole at 20 K. Asterisks indicate impurity signals. Samples with a concentration of about 300 μM were prepared in KPi 50 mM pH 6.8 as detailed in the Supplementary data with 30% of glycerol as glassing agent. (For interpretation of the references to colour in this figure legend, the reader is referred to the web version of this article.)

(not shown), normally associated with the five-coordinate species formed by binding of the substrate with concomitant displacement of the coordinating water. This finding agrees with the crystal structure of CYP116B5hd, which shows a six-coordination of the heme iron where a cysteine residue and a water molecule act as axial ligands [16]. Remarkably, a single species is found in the spectrum reflecting a homogeneous heme environment. The precise *g*-tensor principal values, refined using computer simulations (red trace in Fig. 1), are listed in Table 1 and are compared to P450 BM3 [17], P450cam [7] and P450 with peroxygenase activity [18–20].

The analysis of the *g*-values obtained for CYP116B5hd using the one-hole model (see S.M. Section 2) resulted in values of the crystal-field parameters, Δ/ξ and V/ξ,[1] typical for P450 monooxygenases with cysteine-water coordination (Table 1). The *g*-values of CYP116B5hd differ from those reported for chloroperoxidase and P450 peroxygenases (CYP152), which result in slightly smaller Δ/ξ and considerably smaller V/ξ (see Table 1). In the case of CYP152 peroxygenases, most of the studies report several coexisting EPR species with different degrees of similarity to canonical P450 enzymes or Chloroperoxidase (CPO) (see Table 1). Although the first iron coordination sphere is the same (Cys-H_2O) according to all available structures, a dependence of the *g*-values of low-spin hemeproteins on factors like polarity or charge distribution has been previously described [21,22]. The available substrate-bound crystal structures of CYP152 show that a conserved arginine and the carboxyl group of the fatty acid substrate are very close to the axial water molecule [19,20], configuring a polar distal heme pocket, like CPO and opposed to the generally hydrophobic pockets of typical P450s. Interestingly, the EPR spectrum of another member of the family, CYP152L1 in its substrate-free state, shows several (up to five) low-spin ferric species ranging from the typical P450s to the ones observed for peroxygenases [18] that were attributed to the existence of multiple coordination geometries and hydrogen bonding partners available to the distal water ligand.

The effect of addition of two ligands, histidine and imidazole, on the electronic state of CYP116B5 was then investigated. Upon addition of histidine to the substrate-free protein, a moderate shift in *g*-value was observed (see Fig. 1.b), which translates into a slightly larger Δ/ξ, keeping V/ξ basically unchanged (see Table 1). This small *g*-value shift is consistent with the crystal structure of the protein showing that the carboxylate of a histidine molecule from the crystallization buffer forms a H-bond with the water molecule present as axial ligand [16].

Upon addition of imidazole, known to behave as a Type II ligand for CYP116B5hd,[2] the CW EPR spectrum shows significant changes (Fig. 1c) revealing two new low-spin Fe^{III}-heme species. The *g*-values of one species (2.47, 2.26, 1.86) are slightly shifted with respect to the ones of the substrate-free enzyme (2.44, 2.25, 1.92). While, the other species is characterized by a more anisotropic *g*-tensor (2.58, 2.26, 1.90) with g_z and g_x components falling at lower and higher fields respectively (see arrows in Fig. 1c). Simulation of the two species allowed to obtain their precise *g*-values and to quantify their relative abundance to about (1:1). The *g*-values of both species indicate a modification in the strength of the local coordination environment of the heme centre, as evidenced by a smaller Δ/ξ crystal field parameter, very similar for both species (Table 1). This change could be accounting for the replacement of the water molecule by an imidazole moiety as the distal axial ligand, coordinating the heme iron by means of one of its nitrogen atoms. This interpretation fits with the reported *g*-values for imidazole complexes of P450cam [23]. The most substantial difference between the two imidazole species are the values of V/ξ, which can be attributed to two different conformations of the imidazole molecular plane with respect to the Fe^{III} d orbitals, maintaining approximately the Fe—N distance [26]. The same behaviour is observed upon addition of an excess of imidazole to P450 BM3 (see Table 1 and S.D. Section 1). All these findings suggest that imidazole interferes with the electronic environment of Fe^{III}, possibly displacing the water molecule and coordinating the metal centre. Interestingly, imidazole binding results in g-values in the range reported for CYP152 peroxygenases.

Further characterization of CYP116B5hd, and a direct proof of imidazole binding to the metal centre, came from magnetic field dependent HYSCORE experiments before and after imidazole addition.[3] The X-band HYSCORE spectrum of heme proteins is typically dominated by the presence, in the (−,+) quadrant, of cross-peaks correlating the double quantum transition of nitrogen atoms of the heme ring [12]. For CYP116B5hd in the resting state, the (−,+) quadrant of the spectrum recorded at the g_y magnetic field position (Fig. 2a), is dominated by two cross-peaks symmetrically placed about the diagonal of the negative

[1] [1]Δ/ξ is the energy difference, normalized by the spin-orbit coupling constant (ξ), between d_{xy} orbital and the average of d_{xz} and d_{yz} orbitals of Fe^{III}. This parameter is therefore sensitive to the presence and nature of axial ligands and to the strength of their interaction with the metal. On the other hand, the rhombic parameter, V/ξ, indicates the energy separation of the d_{xz} and d_{yz} orbitals and is related to the nature of the axial ligands and its orientation with respect to the porphyrin ring.

[2] The shift of the Soret peak at 419 nm in the UV-VIS spectrum is often used to determine the interaction of ligands in the P450 active site: a blue shift, to about 416 nm, is interpreted as a low- to high-spin transition and indicates a type I (substrate) ligand while a red shift, to about 425 nm, assesses they act as a type II ligands (inhibitors) directly coordinating the heme. Such kind of tests have been already carried out on CYP116B5hd with several possible substrates and inhibitors, as shown in [6].

[3] A detailed analysis of these spectra will be reported somewhere else, here we will report qualitatively the evidence regarding the distal axial coordination of the iron.

Table 1
g-values of ferric P450 samples, studied in this work, and of other relevant P450 proteins, taken from literature and displayed for comparison. The crystal field parameters Δ/ξ and V/ξ of each protein have been calculated from the corresponding *g*-values [24,25].

.		g_z	g_y	g_x	V/ξ	Δ/ξ	Reference
CYP116B5hd		2.440 ± 0.005	2.25 ± 0.002	1.92 ± 0.002	4.74 ± 0.06	5.44 ± 0.18	This work
P450 BM3		2.418 ± 0.005	2.26 ± 0.002	1.92 ± 0.002	4.98 ± 0.06	5.16 ± 0.017	This work
P450cam		2.45	2.26	1.91	4.59	5.11	[7]
CYP152B1*		2.59	2.25	1.85	3.42	5.15	[19]
CYP152K6*	(1)	2.58	2.25	1.85	3.47	5.10	
	(2)	2.52	2.25	1.87	3.85	5.10	[20]
	(3)	2.47	2.25	1.90	4.35	5.28	
CYP152L1§	(1)	2.55	2.24	1.85	3.59	5.13	[18]
	(2)	2.48	2.24	1.88	4.13	5.22	
CPO		2.62	2.26	1.83	3.24	4.85	[23]
CYP116B5hd + Histidine		2.419 ± 0.005	2.24 ± 0.002	1.92 ± 0.002	4.89 ± 0.06	5.48 ± 0.18	This work
CYP116B5hd + Imidazole	(1)	2.585 ± 0.005	2.26 ± 0.002	1.90 ± 0.002	4.42 ± 0.05	5.14 ± 0.17	This work
	(2)	2.468 ± 0.005	2.26 ± 0.002	1.86 ± 0.002	3.51 ± 0.03	5.12 ± 0.17	
P450 BM3 + Imidazole	(1)	2.450 ± 0.005	2.26 ± 0.002	1.90 ± 0.002	4.53 ± 0.05	4.98 ± 0.17	
	(2)	2.560 ± 0.005	2.26 ± 0.002	1.86 ± 0.002	3.64 ± 0.03	5.05 ± 0.17	This work
	(3)	2.610 ± 0.005	2.26 ± 0.002	1.85 ± 0.002	3.34 ± 0.02	5.01 ± 0.17	

* The crystal structure shows copurification of the enzyme and bound fatty-acid substrate.
§ Up to 5 different species were found in the substrate-free EPR spectrum, only the *g*-values of the most intense ones are reproduced.

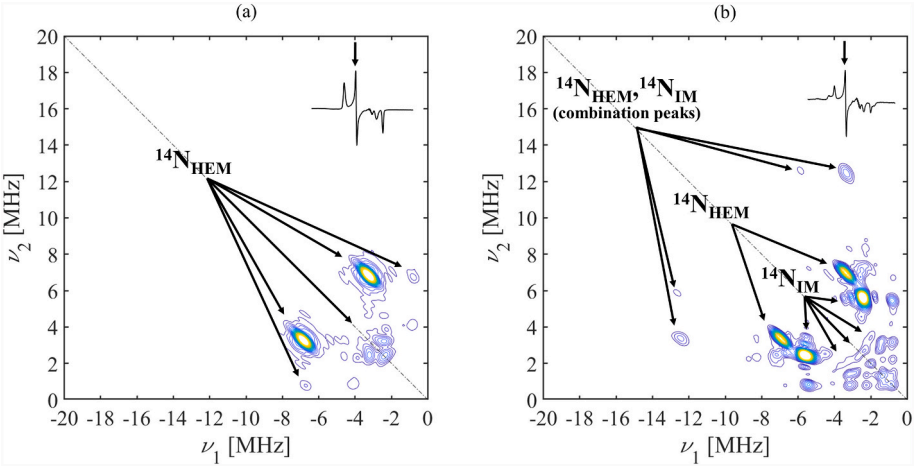

Fig. 2. X-band HYSCORE, only (−,+) quadrant shown, of the spectra of CYP116B5hd frozen solutions recorded at the field position corresponding to the g_y component ($B = 307.9$ mT) (a) CYP116B5hd (b) CYP116B5hd with a 10-fold excess of imidazole. All spectra were recorded at $T = 6$ K and $\tau = 208$ ns. N_{HEM} and N_{IM} indicate the heme and imidazole nitrogen signals respectively. In the inset the magnetic field at which the spectra were recorded is shown in the CW-EPR spectrum.

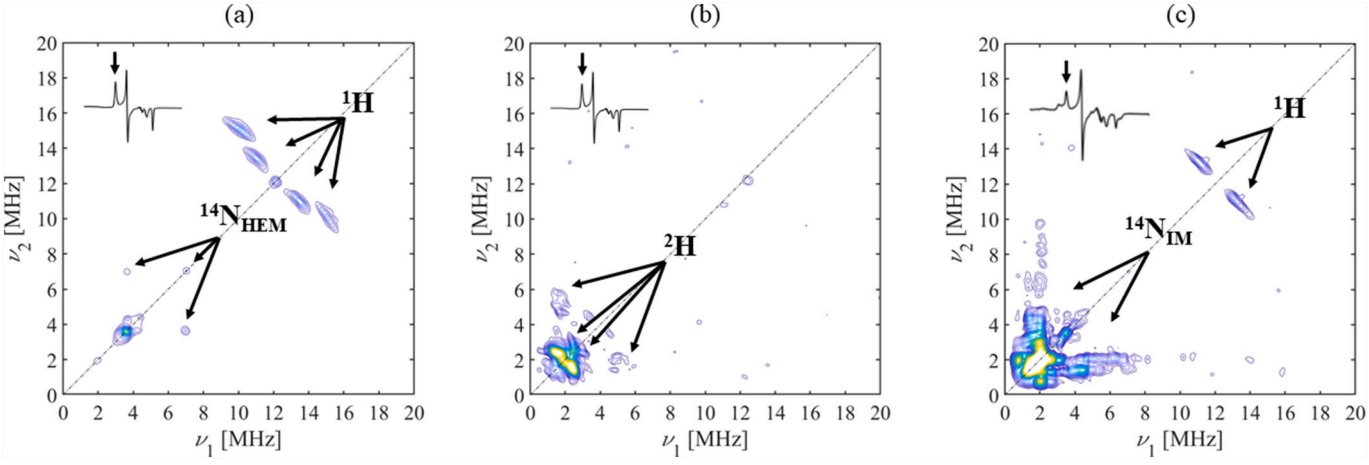

Fig. 3. X-band HYSCORE, only (+,+) quadrant shown, of CYP116B5hd frozen solutions recorded at the magnetic field position corresponding to the g_z component. (a) CYP116B5hd in aqueous buffer ($B = 283.8$ mT, $g_z = 2.44$), (b) CYP116B5hd in deuterated buffer ($B = 290.0$ mT, $g_z = 2.44$) and (c) CYP116B5hd with an excess of imidazole ($B = 283.8$ mT, $g_z = 2.47$). All spectra were recorded at $T = 6$ K and $\tau = 250$ ns. In the inset, the magnetic field at which the spectra were recorded is shown in a CW-EPR spectrum.

quadrant at coordinates (−6.8, 3.2) MHz. They are due to the hyperfine interaction of the electron spin with the heme nitrogen nuclei ($A_{HEM} \sim 5$ MHz) [12,27]. and were therefore labelled as N_{HEM}. X-band HYSCORE experiments recorded at the g_z magnetic field position, in combination with deuterium exchange, provide evidence for a water molecule as the distal axial ligand. Fig. 3a and b show the HYSCORE spectra of ferric CYP116B5hd in a natural and deuterated aqueous buffer, respectively. In the (+,+) quadrant of the natural sample (Fig. 3a), ^{1}H cross-peaks at (15.1 MHz, 10.1 MHz) and (13.5 MHz, 11.0 MHz), due to the interaction of the electron spin with ^{1}H nuclei close to the iron [28,29], are clearly observed, along with peaks at frequencies below 8 MHz assigned to heme ^{14}N nuclei. When the spectrum is recorded with the same experimental conditions in a deuterated buffer (Fig. 3b), we can observe that the proton signals disappear from the spectrum while deuterium correlation peaks dominate the low frequency part of the quadrant.

Spectral simulations of the first set of protons (see S.D.) provide a value of the anisotropic hyperfine coupling compatible with the geometry of bound water.

Upon addition of imidazole, the HYSCORE spectra show two new very intense cross-peaks in the (−,+) quadrant centred at about (−5.6, 2.4) MHz (Fig. 2b). They were assigned to nuclear transitions of a ^{14}N of imidazole (N_{IM} in Fig. 2b) allowing to conclude that the unpaired electron on the Fe^{III} is coupled with both imidazole and heme nitrogens. Estimates of the coupling constants obtained from the ^{14}N peaks ($A_{imid} \sim 4$ MHz) are similar to the interaction parameters obtained for other heme-imidazole systems [12,27]. A significant change is also observed in the (+,+) quadrant (Fig. 3c) where the set of ^{1}H cross-peaks associated to the water ligand is replaced by the typical ^{1}H signal from imidazole hydrogens [12,14], further confirming the substitution of the water molecule by the imidazole azo-compound. Importantly, the ability of HYSCORE to detect the direct coordination of imidazole allows one to discern between two types of cysteine-coordinated heme species with g-values in the range of peroxygenases: one presenting the usual water coordination in a polar environment and the other is coordinated by imidazole as a sixth ligand, which may be present as an impurity from the purification protocol.

Analogous HYSCORE experiments performed for comparison in the heme domain of the reference protein P450 BM3, both in the substrate-free resting state, or after the addition of an excess of imidazole, show practically identical spectra to the ones obtained for CYP116B5hd (see S.D.). This demonstrates that axial water replacement also takes place in the model protein, but most interestingly, it reflects that both proteins not only share practically the same iron ground state (*g*-values) but also have the same unpaired electron density distribution.

Therefore, the EPR characterization shows that, despite its peroxygenase activity, the electronic environment of heme iron in CYP116B5hd in the resting state is closer to the one observed for typical P450 oxidases rather than to peroxygenases and CPO [18–20]. Other factors, such as specific amino acids in the proximal loop and in the electron-transfer pathway, could then be essential for its peroxygenase activity [6] and need to be further explored to better understand the role of protein matrix in P450 reactivity.

Declaration of Competing Interest

The authors declare no conflict of interests.

Acknowledgements

This paper is part of a project that has received funding from the European Union's Horizon 2020 research and innovation programme under the Marie Skłodowska-Curie grant agreement No 813209. The authors would like to acknowledge the use of *Servicio General de Apoyo a la Investigación-SAI, Universidad de Zaragoza* and the support of the Government of Aragón-FEDER (grupo de referencia de Biología Estructural E35-20R).

References

[1] G.A. Roberts, G. Grogan, A. Greter, S.L. Flitsch, N.J. Turner, Identification of a new class of cytochrome P450 from a Rhodococcus sp, J. Bacteriol. 184 (2002) 3898–3908, https://doi.org/10.1128/JB.184.14.3898-3908.2002.

[2] S.C. Hammer, G. Kubik, E. Watkins, S. Huang, H. Minges, F.H. Arnold, Anti-Markovnikov alkene oxidation by metal-oxo–mediated enzyme catalysis, Fundam. Enzym. Eng. 358 (2017) 215–218, https://doi.org/10.1126/science.aao1482.

[3] M. Tavanti, J.L. Porter, S. Sabatini, N.J. Turner, S.L. Flitsch, Panel of new thermostable CYP116B self-sufficient cytochrome P450 monooxygenases that catalyze C − H activation with a diverse substrate scope, ChemCatChem. 10 (2018) 1042–1051, https://doi.org/10.1002/cctc.201701510.

[4] D. Correddu, G. Di Nardo, G. Gilardi, Self-sufficient class VII cytochromes P450: from full-length structure to synthetic biology applications, Trends Biotechnol. (2021), https://doi.org/10.1016/j.tibtech.2021.01.011.

[5] D. Minerdi, S.J. Sadeghi, G. Di Nardo, F. Rua, S. Castrignanò, P. Allegra, G. Gilardi, CYP116B5: a new class VII catalytically self-sufficient cytochrome P450 from *A. radioresistens* that enables growth on alkanes, Mol. Microbiol. 95 (2015) 539–554, https://doi.org/10.1111/mmi.12883.

[6] A. Ciaramella, G. Catucci, G. Di Nardo, S.J. Sadeghi, G. Gilardi, Peroxide-driven catalysis of the heme domain of A . radioresistens cytochrome P450 116B5 for sustainable aromatic rings oxidation and drug metabolites production, New Biotechnol. 54 (2020) 71–79, https://doi.org/10.1016/j.nbt.2019.08.005.

[7] J.D. Lipscomb, Electron paramagnetic resonance detectable states of cytochrome P-450Cam, Biochemistry. 19 (1980) 3590–3599, https://doi.org/10.1021/bi00556a027.

[8] H. Thomann, M. Bernardo, D. Goldfarb, P.M.H. Kroneck, V. Ullrich, Evidence for water binding to the fe center in cytochrome modulation spectroscopy, J. Am. Chem. Soc. 117 (1995) 8243–8251, https://doi.org/10.1021/ja00136a023.

[9] R. Davydov, T.M. Makris, V. Kofman, D.E. Werst, S.G. Sligar, B.M. Hoffman, Hydroxylation of camphor by reduced oxy-cytochrome p450cam: mechanistic implications of EPR and ENDOR studies of catalytic intermediates in native and mutant enzymes, J. Am. Chem. Soc. 123 (2001) 1403–1415, https://doi.org/10.1021/ja003583l.

[10] C. Aldag, I.A. Gromov, I. García-Rubio, K. Von Koenig, I. Schlichting, B. Jaun, D. Hilvert, Probing the role of the proximal heme ligand in cytochrome P450cam by recombinant incorporation of selenocysteine, Proc. Natl. Acad. Sci. U. S. A. 106 (2009) 5481–5486, https://doi.org/10.1073/pnas.0810503106.

[11] J. Rittle, M.T. Green, Cytochrome P450 compound I: Capture, characterization, and C—H bond activation kinetics, Science (80-.) 330 (2010) 933–937, https://doi.org/10.1126/science.1193478.

[12] I. García-Rubio, J.I. Martínez, R. Picorel, I. Yruela, P.J. Alonso, HYSCORE spectroscopy in the cytochrome b559 of the photosystem II reaction center, J. Am. Chem. Soc. 125 (2003) 15846–15854, https://doi.org/10.1021/ja035364g.

[13] E. Vinck, S. Van Doorslaer, S. Dewilde, G. Mitrikas, A. Schweiger, L. Moens, Analyzing heme proteins using EPR techniques: the heme-pocket structure of ferric mouse neuroglobin, J. Biol. Inorg. Chem. 11 (2006) 467–475, https://doi.org/10.1007/s00775-006-0100-2.

[14] I. García-Rubio, P.J. Alonso, M. Medina, J.I. Martínez, Hyperfine correlation spectroscopy and electron spin echo envelope modulation spectroscopy study of the two coexisting forms of the hemeprotein cytochrome c6 from Anabaena Pcc7119, Biophys. J. 96 (2009) 141–152, https://doi.org/10.1529/biophysj.108.133272.

[15] I. García-Rubio, G. Mitrikas, Structure and spin density of ferric low-spin heme complexes determined with high-resolution ESEEM experiments at 35 GHz, J. Biol. Inorg. Chem. 15 (2010) 929–941, https://doi.org/10.1007/s00775-010-0655-9.

[16] A. Ciaramella, G. Catucci, G. Gilardi, G. Di, Crystal structure of bacterial CYP116B5 heme domain: New insights on class VII P450s structural flexibility and peroxygenase activity, Int. J. Biol. Macromol. 140 (2019) 577–587, https://doi.org/10.1016/j.ijbiomac.2019.08.141.

[17] H.M. Girvan, K.R. Marshall, R.J. Lawson, D. Leys, M.G. Joyce, J. Clarkson, W. E. Smith, M.R. Cheesman, A.W. Munro, Flavocytochrome P450 BM3 mutant A264E undergoes substrate-dependent formation of a novel heme iron ligand set, J. Biol. Chem. 279 (2004) 23274–23286, https://doi.org/10.1074/jbc.M401716200.

[18] J. Belcher, K.J. McLean, S. Matthews, L.S. Woodward, K. Fisher, S.E.J. Rigby, D. R. Nelson, D. Potts, M.T. Baynham, D.A. Parker, D. Leys, A.W. Munro, Structure and biochemical properties of the alkene producing cytochrome *p*450 OleTJE (CYP152l1) from the jeotgalicoccus sp. 8456 bacterium, J. Biol. Chem. 289 (2014) 6535–6550, https://doi.org/10.1074/jbc.M113.527325.

[19] T. Fujishiro, O. Shoji, S. Nagano, H. Sugimoto, Y. Shiro, Y. Watanabe, Crystal structure of H 2O 2-dependent cytochrome P450 SPαwith its bound fatty acid substrate: Insight into the regioselective hydroxylation of fatty acids at the α position, J. Biol. Chem. 286 (2011) 29941–29950, https://doi.org/10.1074/jbc.M111.245225.

[20] H.M. Girvan, H. Poddar, K.J. McLean, D.R. Nelson, K.A. Hollywood, C.W. Levy, D. Leys, A.W. Munro, Structural and catalytic properties of the peroxygenase P450 enzyme CYP152K6 from *Bacillus methanolicus*, J. Inorg. Biochem. 188 (2018) 18–28, https://doi.org/10.1016/j.jinorgbio.2018.08.002.

[21] I. Yruela, I. García-Rubio, M. Roncel, J.I. Martínez, M.V. Ramiro, J.M. Ortega, P. J. Alonso, R. Picorel, Detergent effect on Cytochrome b559 electron paramagnetic resonance signals in the photosystem II reaction centre, Photochem. Photobiol. Sci. 2 (2003) 437–442, https://doi.org/10.1039/b300187c.

[22] P. Bernal-Bayard, L. Puerto-Galán, I. Yruela, I. García-Rubio, C. Castell, J. M. Ortega, P.J. Alonso, M. Roncel, J.I. Martínez, M. Hervás, J.A. Navarro, The photosynthetic cytochrome *c* 550 from the diatom *Phaeodactylum tricornutum*,

Photosynth. Res. 133 (2017) 273–287, https://doi.org/10.1007/s11120-016-0327-x.
[23] M. Sono, L.P. Hager, J.H. Dawson, Electron paramagnetic resonance investigations of exogenous ligand complexes of low-spin ferric chloroperoxidase: further support for endogenous thiolate ligation to the heme iron, Biochim. Biophys. Acta (BBA)/Protein Struct. Mol. 1078 (1991) 351–359, https://doi.org/10.1016/0167-4838(91)90156-T.
[24] C.P.S. Taylor, The EPR of low spin heme complexes Relation of the t2g hole model to the directional properties of the g tensor, and a new method for calculating the ligand field parameters, BBA - Protein Struct. 491 (1977) 137–148, https://doi.org/10.1016/0005-2795(77)90049-6.
[25] P.J. Alonso, J.I. Martínez, I. García-Rubio, The study of the ground state Kramers doublet of low-spin heminic system revisited. A comprehensive description of the EPR and Mössbauer spectra, Coord. Chem. Rev. 251 (2007) 12–24, https://doi.org/10.1016/j.ccr.2006.05.007.
[26] I. García-Rubio, M. Medina, R. Cammack, P.J. Alonso, J.I. Martínez, CW-EPR and ENDOR study of cytochrome *c*6 from Anabaena PCC 7119, Biophys. J. 91 (2006) 2250–2263, https://doi.org/10.1529/biophysj.105.080358.
[27] E. Vinck, S. Van Doorslaer, Analyzing low-spin ferric complexes using pulse EPR techniques: a structure determination of bis (4-methylimidazole) (tetraphenylporphyrinato)iron(III), Phys. Chem. Chem. Phys. 6 (2004) 5324–5330, https://doi.org/10.1039/b411444b.
[28] D. Goldfarb, M. Bernardo, H. Thomann, P.M.H. Kroneck, V. Ullrich, Study of water binding to low-spin Fe(III) in cytochrome P450 by pulsed ENDOR and four-pulse ESEEM spectroscopies, J. Am. Chem. Soc. 118 (1996) 2686–2693, https://doi.org/10.1021/ja951307e.
[29] K.P. Conner, P. Vennam, C.M. Woods, M.D. Krzyaniak, M.K. Bowman, W.M. Atkins, 1,2,3-Triazole-heme interactions in cytochrome P450: functionally competent triazole-water-heme complexes, Biochemistry. 51 (2012) 6441–6457, https://doi.org/10.1021/bi300744z.